Ceduna-1 Survey

M.Kesteven & B. Parsons

11 October 1996

1 Summary

The Ceduna-1 antenna was surveyed at the zenith on October 1. There are a number of puzzling aspects to the survey, so a detailed analysis of the survey technique and the likely errors is given. The antenna is probably no worse than 2.5mm (half-path rms).

The stability of the structure as a function of elevation was tested - the preliminary indications are that the subreflector moves about 20mm as the antenna tips from zenith to horizon; the reflector surface also deforms, shortening the focal length as the elevation decreases.

2 Introduction

The Ceduna-1 antenna operated for many years as a communications antenna at a low elevation, at frequencies 4 to 6 GHz. With its reincarnation as a radiotelescope the question arises as to its suitability for high frequency all-sky operation. A tape and theodolite survey measured the figure of the reflector at one elevation (the zenith). A second experiment using a video camera measured the deformation of the structure as a function of elevation.

3 The Tape and Theodolite Survey

3.1 Targets

The targets are placed on the surface at known distances from the theodolite. We use a semi-rigid tape attached to a collar which is concentric with the theodolite's axis. The targets are fine pencil marks laid directly on the panel surface; cursors bolted to the tape provide the accurate guide for the pencil. The cursors were positioned on the tape against marks previously scribed on the tape surface. The first 10m of the tape had previously been marked for the Narrabri antennas, with tape marks calibrated in the NML tape tunnel; the marks on the outer 6m were measured at Epping. Bear in mind that for this survey we were not required to place the targets near the panel adjustment points, since our aim was to assess the surface precision. A new set of tape marks would indeed need to be tailored explicitly for the Ceduna antenna should a surface adjustment be necessary.

Figure 1 shows the panel layout and the target locations.

We chose a semi-rigid tape in order to ensure that the targets are positioned at precisely defined arc lengths from the antenna vertex (defined by the theodolite position). The final step in this preparation is to compute a table of target positions in terms of theodolite azimuth and elevation settings - these

settings will subsequently be compared with the actual theodolite readings in the survey analysis. The computation is based on the reflector profile provided by Mitsubishi, and attached as appendix A.

3.2 Target Setting

Most targets were marked on september 30, in the late afternoon. The weather was overcast, cold and windy. Rain set in before the operation was complete, and the targets in the azimuth range 330-357 degrees were marked the following morning.

3.3 Observations

A pilot run on ring #5 was made in the late morning of Oct. 1. The weather was variably overcast and sunny. The full survey was made from 8pm to midnight on Oct. 1.

We used ring #5 as the reference ring - a selected sub-set of its targets was re-observed throughout the survey period to monitor shifts in the structure (none were found).

The weather during the survey was cold, damp and miserable. There was no wind, but there was heavy dew.

4 Analysis

The analysis is simple: we compare the observed target elevation with the predicted elevation. We check the data (the differences) for the signatures of systematic errors - a tilt in the theodolite axis, for example, will impose a sinusoid(azimuth) pattern in the differences; a vertical shift in the theodolite will affect each ring of targets in a predictable manner. We can elect to correct the data for any systematic errors, with the residue attributed to panel setting errors. Table I summarises the systematic errors, and table II summarises the panel setting errors.

Table I - The systematic error signatures

ring	axis tilt (asec)	axis az. (degree)	theodolite shift (vertical) (mm)
1	50	326	1.40
2	21	261	1.76
3	19	191	2.19
4	19	223	1.51
5	18	203	0.85
6	11	237	-0.45
7	15	223	0.55
8	15	228	-2.33
9	9	221	-2.13
10	14	31	-7.66
mean	8.3	231	-0.4

Notes: Column 4 ("Theodolite shift") is computed from the difference between the mean elevation of a ring of targets and the theoretical elevation for that ring. The difference could be attributed to an

error in the axial position of the theodolite, or equivalently to a systematic error in the entire ring. If the theodolite is indeed in error, then the same shift should be seen in all target rings; if the antenna does not conform to the nominal profile then the shift could vary from ring to ring, as is the case here.

Table II - The Panel Setting Errors

ring	single ring rms (mm)	full dish rms (mm)	half-path rms (mm)
1	0.31	1.91	1.90
2	0.40	2.25	2.22
3	0.56	2.71	2.63
4	0.56	2.04	1.95
5	0.77	1.53	1.41
6	0.99	1.00	0.89
7	1.26	1.63	1.39
8	1.54	2.55	2.13
9	1.65	2.45	1.99
10	2.35	8.11	6.28

Notes: Column 2 is the panel setting error when each ring is considered in isolation, assuming that the mean ring height is correctly set to the profile; column 3 is the better measure, showing the panel rms relative to the best fit paraboloid. Column 4 is the value to use in a Ruze-type gain expression.

Figure 2 shows the setting errors for all targets; each target ring is offset from its neighbor by 2 mm.

These results are disappointing, particularly when viewed against the high quality evident in the construction of the antenna. Since there are a number of large-scale systematic effects present, it is important to check that the problems are antenna-based, and not survey-based.

4.1 The Problems

1. The antenna does not appear to conform to the specified profile. This is evident in the "theodolite shift" which varies from ring to ring.
2. The outer 6 rings of targets have a similar profile in azimuth. It is this common profile which has raised the rms of each ring.

5 Detailed Scrutiny of the Survey

5.1 Theodolite Pointing

The observation protocol includes a check for theodolite collimation - we observe each ring of targets in FACE I mode (in effect, on the 0-180 degree elevation sector), then repeat the observations on FACE II (180-360 sector). The mean of the two readings/target will cancel any collimation error; the **difference** is a measure of the theodolite collimation; the rms of the collimation values is our quality index - it is the rms of the theodolite pointing error.

We find for this survey that the error of a single pointing is 3 arcseconds (rms).

We observed ring #5 twice - once during the day, and in the full survey (at about midnight). Figure 3 shows the data; the correlation is excellent, providing a further measure of confidence in our technique.

We conclude that the intrinsic accuracy of the observations is high and unlikely to contribute to the problems.

5.2 The Theodolite Support Beam

The theodolite was positioned on a beam which straddled the central hub. The beam (even after work to strengthen it) still exhibited a degree of flexibility. Great care was taken during the observations to ensure that the beam was free when each datum was recorded. Tests showed that casual leaning on the beam could shift the sightline by $\sim$ 20 asec. The pointing results confirm that our precautions were adequate.

5.3 Are the Tape Marks Incorrectly placed ?

The analysis appears to show that the antenna's profile is not correct - see column 4 of table I.

An alternative explanation could lie in incorrect marking of the tape. The required errors are large, as shown in Table III; we are confident that we can read a tape to better accuracy. As an additional precaution we measured the diameters of each ring of targets. The measurements were made in the "N-S" plane, with an error of 1-2mm. This data is also included in Table III. We conclude that the problem lies with the antenna - the implied errors in the tape marks are well outside our measurement errors; the implied radii are consistent with our measured radii.

Table III - Alternative views of the error in the mean elevation.

				Implied	
ring	radius (mm)	Δ Rad (mm)	Δ y (mm)	Δ Rad (mm)	Δ y (mm)
1	1766	-	1.4	0.13	5.6
2	2976	1.6	1.8	0.27	8.9
3	4526	0.8	2.2	0.49	11.0
4	5730	0.3	1.5	0.43	7.2
5	7764	0.7	0.9	0.35	3.6
6	9419	-1.5	-0.5	-0.24	-1.8
7	11081	0.9	0.6	0.33	2.0
8	12264	-0.4	-2.3	-1.4	-8.3
9	13416	0.7	-2.1	-1.4	-7.3
10	14775	-7.1	-7.7	-5.7	-24.0
	[2]	[3]	[4]	[5]	[6]

Notes: Column 3 is the difference between the theoretical radius (set by the arc length and the radial profile) and the measured radius. Column 4 is the height error (column 4 of Table I). Column 5 has the implied radius error - the error one should measure if the problem (column 4) arose because the focal length of the reflector had changed. Column 6 has the implied tape error - the magnitude of the error in marking the tape. Column 5 is consistent within errors with column 3; column 6 is not consistent with our ability to mark and measure the tape.

summary #1

- There is a small change in the focal length of the antenna, of around 10mm.

- Relative to the revised profile (extended focal length) the ring-to-ring rms is 0.7mm.

5.4 Why do all the rings have the same profile ?

It is clear in figure 2 that the outer profiles are very similar. This is shown is greater detail in figs. 4-6. The correlation coefficient between adjacent profiles is high (0.8 to 0.95). This suggests strongly that the large rms of each profile is a property of the antenna - and not one of measurement error. And clearly, it is not a random point-to-point error.

Examination of figs. 4-6 shows that the error is essentially a constant angular error (60 asec in all the outer rings); very much as if the antenna had been adjusted by sectors, rather than by azimuth, with the consequent danger of a theodolite axis shift between sectors.

The very high correlation between the two surveys of ring #5 shows that the problem is not a temperature effect, nor is it likely that the observer's weight has imposed a shifting distortion.

6 Conclusion

- The antenna's surface has an overall half-path rms of around 2.8mm, and a 3dB frequency of 8 GHz.
- The error is concentrated in two sectors - around azimuth 150 and azimuth 230.
- The error distribution is not symmetric about the N-S plane - that is, it is not likely to be a gravitational bias, since the structure is symmetrical to a high degree.

7 Structural Stability

We used a variant of the Parkes camera technique to measure the dish deformations. The targets were black 20mm diameter circles placed on a white background; the images were captured by a video camera connected to a frame-grabber in a PC. The camera was fixed to the structure at the vertex; its zoom capability gave us a resolution of 2 pixels/mm for the targets studied. The high contrast allowed us to threshold the image, and process the image on-line; the program searched the image for the white $->$ black transitions in the image, then fitted a circle to the contour. Tests had demonstrated a positioning accuracy of 0.5mm over 10m distances.

Some difficulties were encountered in our first trials: the camera mount proved insufficiently stable; a new mount was assembled which was adequate for this pilot study, but further work is required.

The experiment was curtailed after a power failure at the site.

At this stage we have good data on two targets (subreflector and the dish surface, 9m from the vertex, adjacent to the North tripod leg); we have data of lesser quality for two additional targets on the surface, South and West, at 9m.

The data are shown in fig. 7, along with a (1-COS(elevation)) fit.

8 Discussion

The data are preliminary, as some further work is required to understand and calibrate the camera. The evidence points to a subreflector droop of 20mm as the antenna tips from the zenith to the

horizon. The surface deformation, at the radius of the tripod legs seems more like 10mm, in the sense of reducing the focal length at lower elevations.

We have no data at this stage to indicate the movement (if any) of the vertex of the best fit paraboloid.

9 Conclusion and Recommendations

- The overall half-path rms is 2.85mm. The major contributors to this error are the large-scale departures from the given profile.
- The antenna deforms with elevation - the apparent subreflector droop is around 20mm, while the surface movement is probably a bit less.
- A comprehensive study of the deformations would be advisable before a surface resetting were contemplated - this would clarify the extent to which the movement is homologous, which then defines the surface adjustment goals.
- Resetting the surface to an rms of 0.5mm would likely require 2 to 3 survey/adjustment iterations, and probably take two weeks.

Pg 7. Appendix A - not for distribution

11 Appendix B

Panel setting errors - the details

data NOT CORRECTED for tilt and height

(negative means adjust down).

Ring 1

Panel	Inner		Outer	
	left	right	left	right
	(all adjustments in mm)			
1	-1.3	-2.0	-1.3	-1.4
3	-1.6	-1.7	-1.7	-1.5
5	-0.9	-1.4	-1.6	-1.2
7	-1.6	-1.2	-1.5	-0.8
9	-0.6	-1.5	-1.6	-2.7
11	-0.8	-0.8	-2.0	-1.9
13	-1.4	-0.9	-1.9	-1.1
15	-0.9	-1.6	-2.0	-1.9
17	-1.7	-1.5	-1.9	-2.0
19	-2.3	-1.5	-2.7	-1.9
21	-1.5	-1.9	-2.1	-1.8
23	-2.1	-2.0	-2.7	-1.8

RMS Setting error for this ring : 1.69 mm
RMS half-path error for this ring : 1.67 mm

Ring 2

Panel	Inner		Outer	
	left	right	left	right
	(all adjustments in mm)			
1	-2.1	-0.9	-0.9	0.0
3	-1.5	-1.0	0.2	-2.0
5	-1.6	-2.2	-0.7	-1.2
7	-2.5	-1.8	-1.3	-1.3
9	-2.3	-3.7	-1.3	-1.6
11	-3.1	-3.1	-2.2	-2.0
13	-2.6	-2.1	-2.4	-1.4
15	-2.5	-2.0	-2.0	-1.5
17	-1.8	-2.4	-1.8	-2.0
19	-2.2	-2.0	-2.0	-1.8
21	-2.8	-2.8	-2.2	-1.7
23	-2.2	-2.7	-1.3	-2.7

RMS Setting error for this ring : 2.03 mm
RMS half-path error for this ring : 1.96 mm

Ring 3

Panel	Inner		Outer	
	left	right	left	right
	(all adjustments in mm)			
1	0.4	0.9	0.8	1.8
3	0.1	0.9	2.3	2.7
5	1.0	0.1	2.2	2.2
7	0.4	0.3	1.8	1.6
9	-0.3	-0.1	0.7	1.8
11	-0.9	-0.2	-0.2	-0.0
13	-0.9	-0.9	0.8	1.1
15	-0.8	-1.5	1.1	1.3
17	-0.7	-1.8	0.7	-0.4
19	-2.7	-2.1	-0.2	-0.6
21	-2.7	-2.1	-0.6	-0.9
23	-1.8	-1.4	-0.8	-0.4
25	-1.0	-1.6	-0.5	0.2
27	-0.4	-0.4	1.2	1.0
29	-0.2	-0.6	1.5	1.4
31	0.0	-0.9	0.6	1.5
33	-0.8	-1.3	1.1	0.6
35	-1.5	-1.6	0.9	0.2
37	-2.5	-1.6	-0.5	-0.6
39	-2.0	-0.9	-2.0	-1.4
41	-2.0	-1.6	-0.3	0.0
43	-1.7	-0.8	-0.0	-0.1
45	-0.5	-0.3	0.1	0.3
47	-0.4	-0.6	-1.3	-0.5

RMS Setting error for this ring : 1.21 mm
RMS half-path error for this ring : 1.10 mm

Ring 4

Panel	Inner		Outer	
	left	right	left	right
	(all adjustments in mm)			
1	-1.3	1.2	3.5	4.0
3	1.3	2.7	4.1	5.1
5	2.3	1.5	5.7	5.2
7	0.5	1.5	4.2	4.1
9	0.7	-0.1	3.9	3.9
11	-0.0	-0.0	3.5	3.1
13	-0.4	0.9	3.8	2.8
15	0.2	0.1	3.7	2.6
17	-0.5	-1.3	2.8	2.3
19	-1.8	-2.6	0.3	-0.2
21	-2.2	-3.1	-0.5	-0.3
23	-2.4	-2.3	0.5	1.1
25	-2.3	-1.0	0.4	1.8

27	-0.4	0.1	3.1	3.3
29	-0.6	0.5	2.9	3.7
31	1.5	0.9	4.5	4.2
33	-0.7	-0.3	3.6	3.6
35	-0.2	-0.8	2.5	1.9
37	-1.7	-1.9	0.7	0.9
39	-3.0	-2.1	-1.3	0.3
41	-2.0	-1.8	0.3	0.3
43	-1.6	-1.3	1.2	1.9
45	-1.6	-0.4	2.1	1.9
47	-1.4	-0.5	2.0	1.4

RMS Setting error for this ring : 2.35 mm
RMS half-path error for this ring : 1.97 mm

Ring 5

Panel	Inner		Outer	
	left	right	left	right
	(all adjustments in mm)			
1	3.1	4.4	7.5	7.8
3	3.4	5.7	9.9	10.8
5	3.6	5.1	11.2	10.3
7	3.1	3.1	7.8	7.6
9	2.2	3.7	9.4	7.4
11	2.9	3.7	5.7	6.6
13	3.5	2.7	6.9	8.7
15	2.7	3.3	8.1	7.6
17	3.1	2.6	7.3	7.8
19	-0.6	-0.9	3.7	6.5
21	-0.5	0.2	4.6	4.4
23	-1.0	0.5	8.3	8.6
25	-0.0	2.0	10.4	8.7
27	1.5	4.2	9.5	10.9
29	3.7	5.0	10.3	12.9
31	4.3	4.1	14.4	13.0
33	3.7	2.9	12.6	11.2
35	2.9	2.3	11.0	8.3
37	0.8	0.4	6.1	6.4
39	-0.6	-0.1	6.9	5.4
41	0.0	1.1	5.2	5.2
43	1.1	2.3	5.6	5.8
45	0.8	2.1	5.9	6.4
47	1.3	1.5	5.5	5.5

RMS Setting error for this ring : 6.30 mm
RMS half-path error for this ring : 4.90 mm

Overall RMS setting error : 3.54 mm

Overall RMS half-path error : 2.85 mm

Figure Captions

Figure 1 Panel and target layout.

Figure 2 The panel setting errors. All 10 rings of targets are shown. The vertical scale is marked in mm. Each ring is offset from its neighbor by 2mm, with ring 1 at the top.

Figures 3 to 6 all have the same format: each has four panels comparing two rings of targets. The top left has the first ring; the lower left has the second ring; in addition, the first ring is replotted, offset to the elevation of the second ring. The addition is marked with crosses. The top right panel shows the correlation between the two rings; the data shown are the offsets, in arcseconds, relative to the mean elevation. The lower right panel has the difference between the two curves of the lower left panel.

Figure 3 compares the daytime observation of ring #5 (R5/1) with the night-time observation (R5/2)

Figure 4 compares rings 5 and 6.

Figure 5 compares rings 7 and 8

Figure 6 compares rings 9 and 10.

Figure 7 shows the deformation, as a function of elevation, for two locations: the subreflector (upper panel), and the surface 9m from the vertex, below the upper tripod leg. The vertical axis is marked in mm.

Ceduna–1. Panel and Target layout

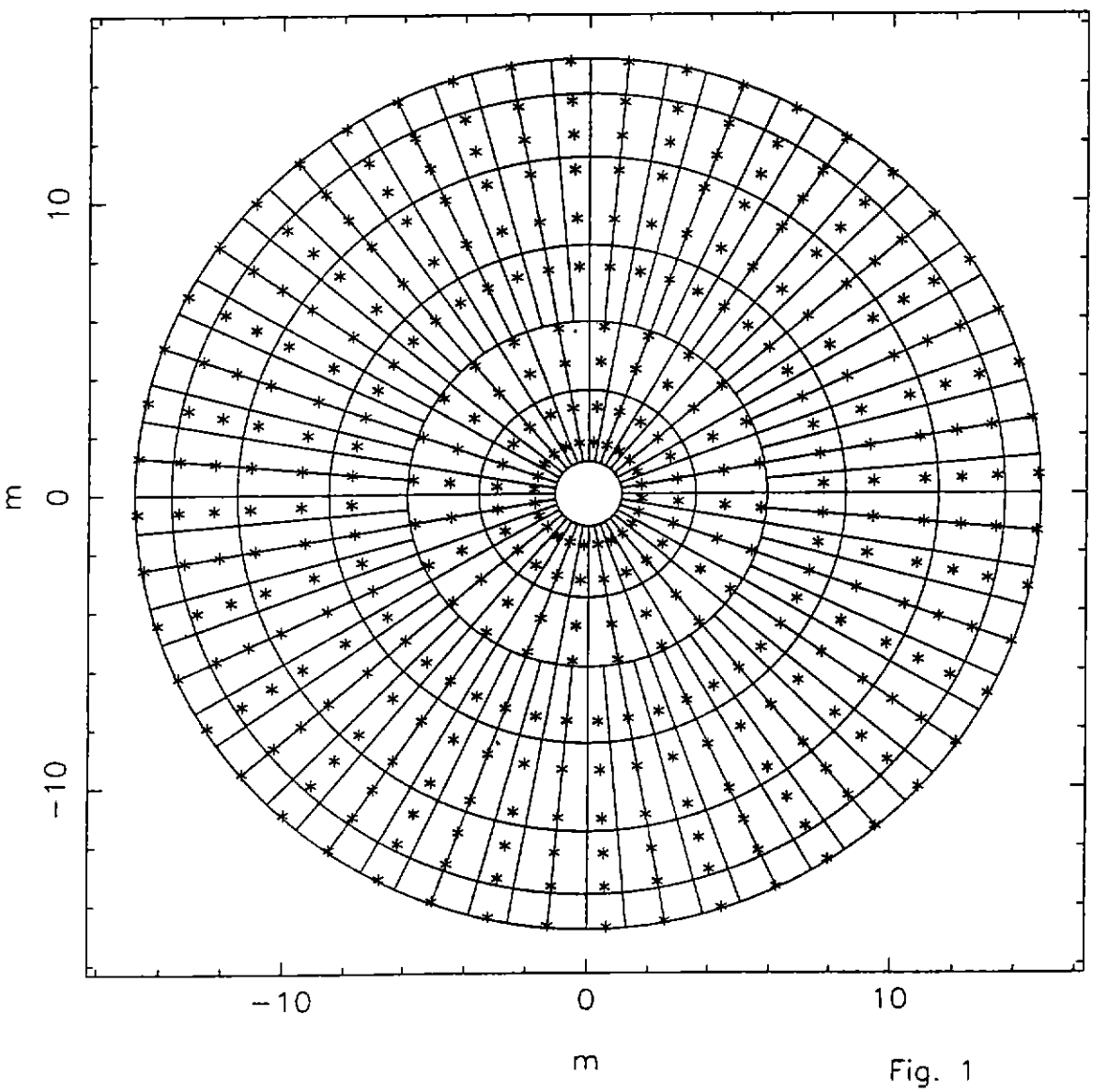

Fig. 1

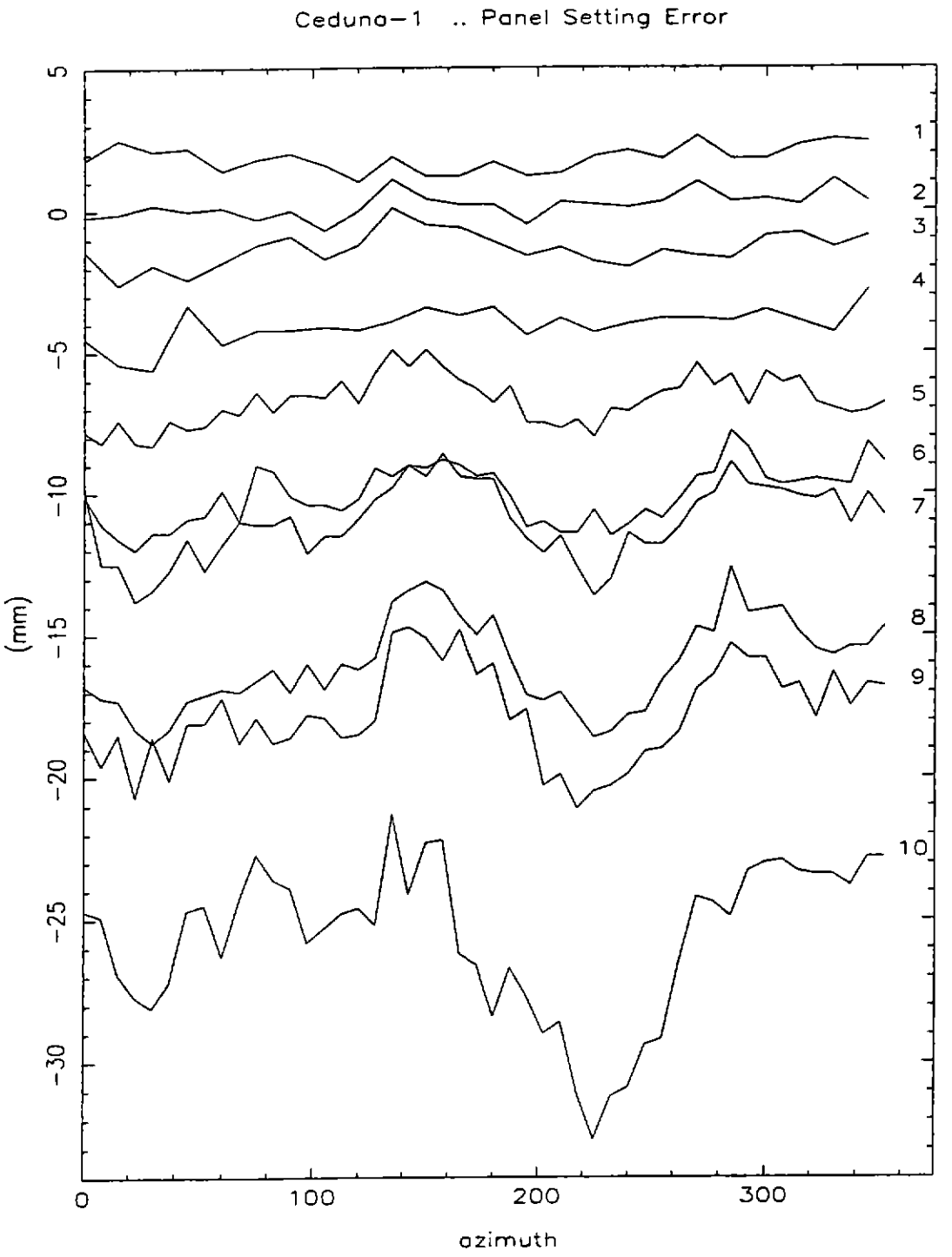
Ceduna–1 .. Panel Setting Error
5
0
-5
-10
-15
-20
-25
-30
(mm)
1
2
3
4
5
6
7
8
9
10
0
100
200
300
azimuth

Fig. 2

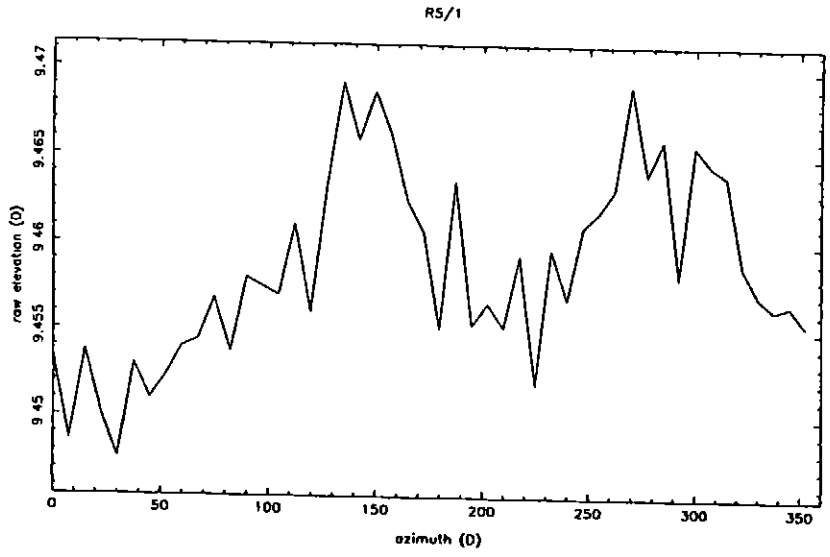
R5/1
raw elevation (D)
9.47
9.465
9.46
9.455
9.45
0
50
100
150
200
250
300
350
azimuth (D)

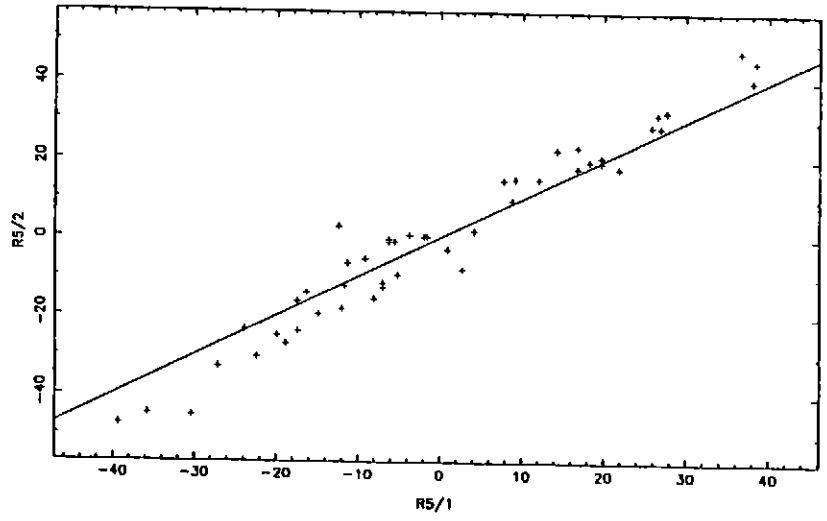
R5/2
40
20
0
-20
-40
-40
-30
-20
-10
0
10
20
30
40
R5/1

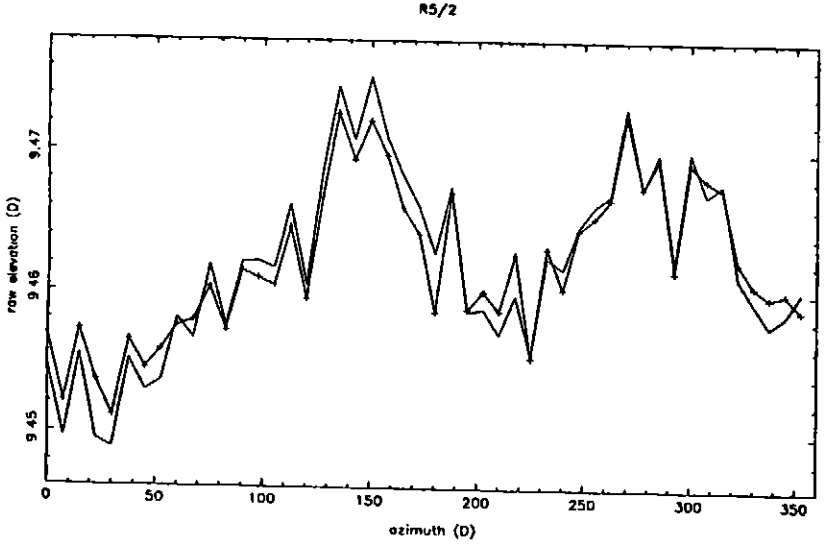
R5/2
raw elevation (D)
9.47
9.46
9.45
0
50
100
150
200
250
300
350
azimuth (D)

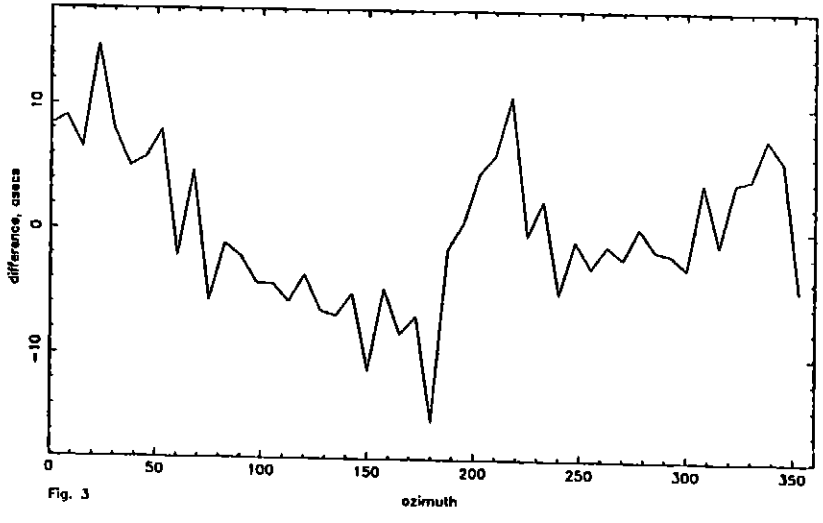
difference, asecs
10
0
-10
0
50
100
150
200
250
300
350
azimuth

Fig. 3

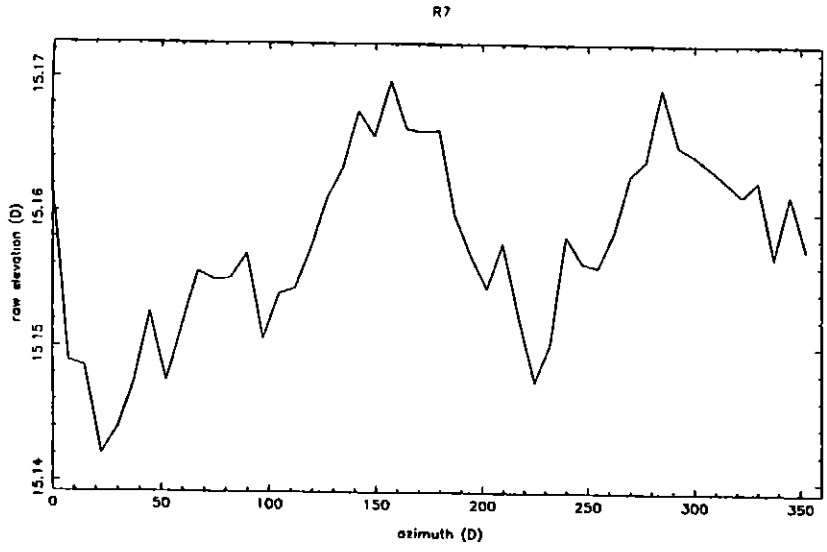
R7
raw elevation (D)
15.17
15.16
15.15
15.14
0
50
100
150
200
250
300
350
azimuth (D)

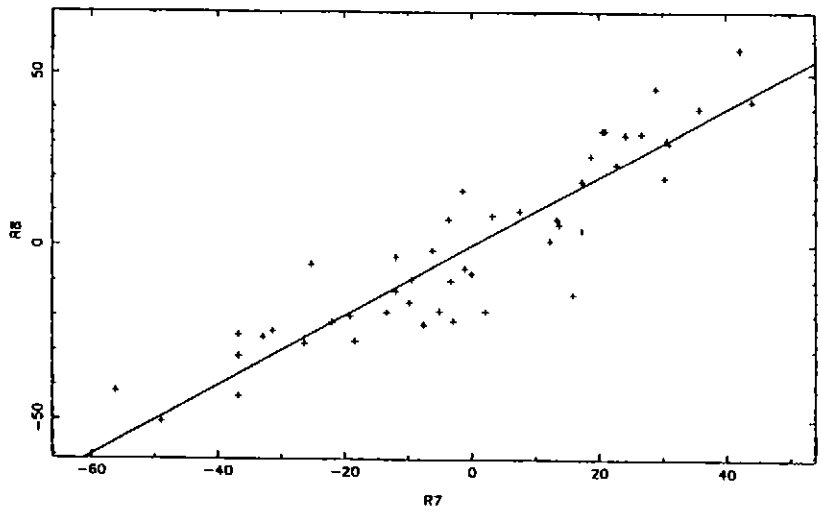
R8
50
0
-50
-60
-40
-20
0
20
40
R7

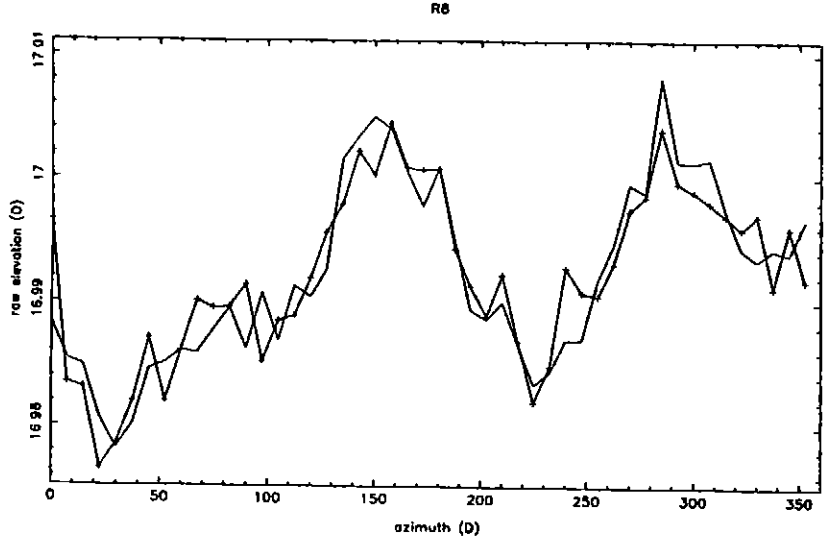
R8
raw elevation (D)
17.01
17
16.99
16.98
0
50
100
150
200
250
300
350
azimuth (D)

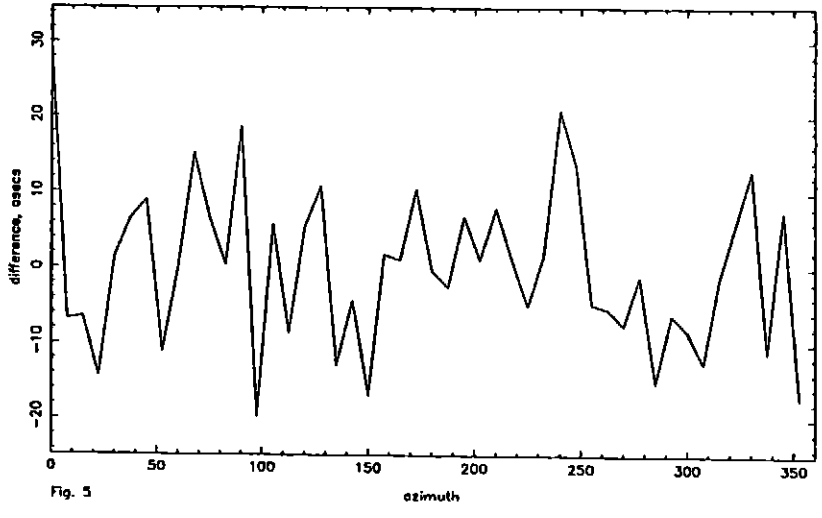
difference, asecs
30
20
10
0
-10
-20
0
50
100
150
200
250
300
350
azimuth

Fig. 5

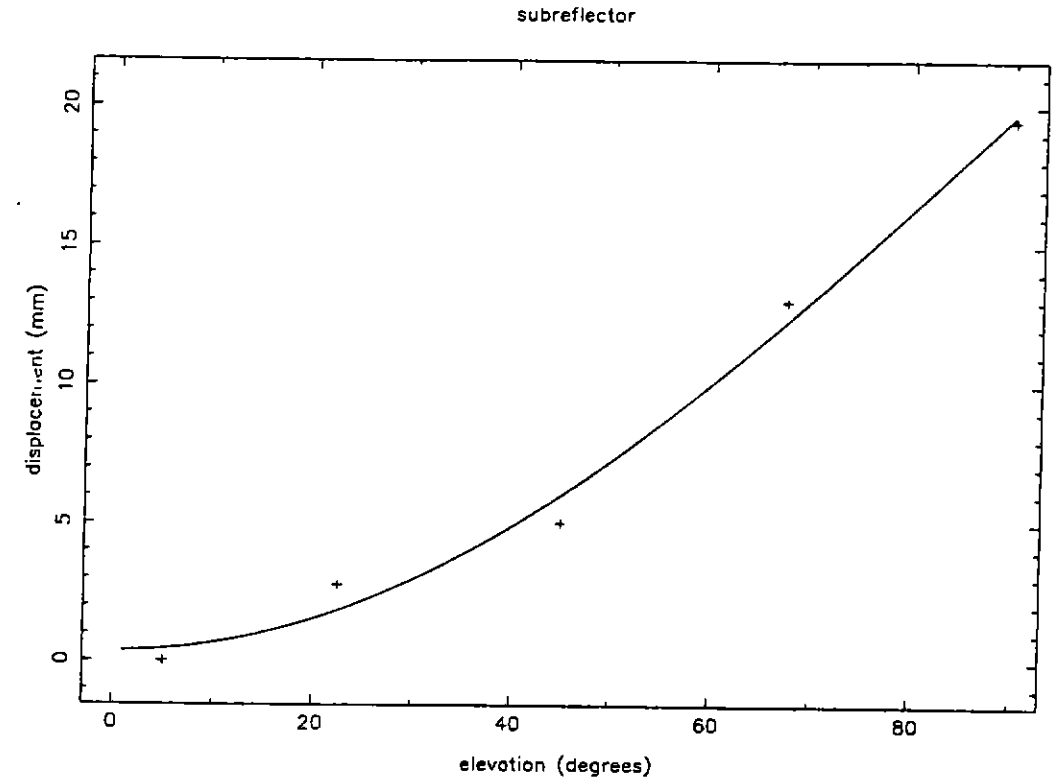
subreflector
displacement (mm)
0
5
10
15
20
0
20
40
60
80
elevation (degrees)

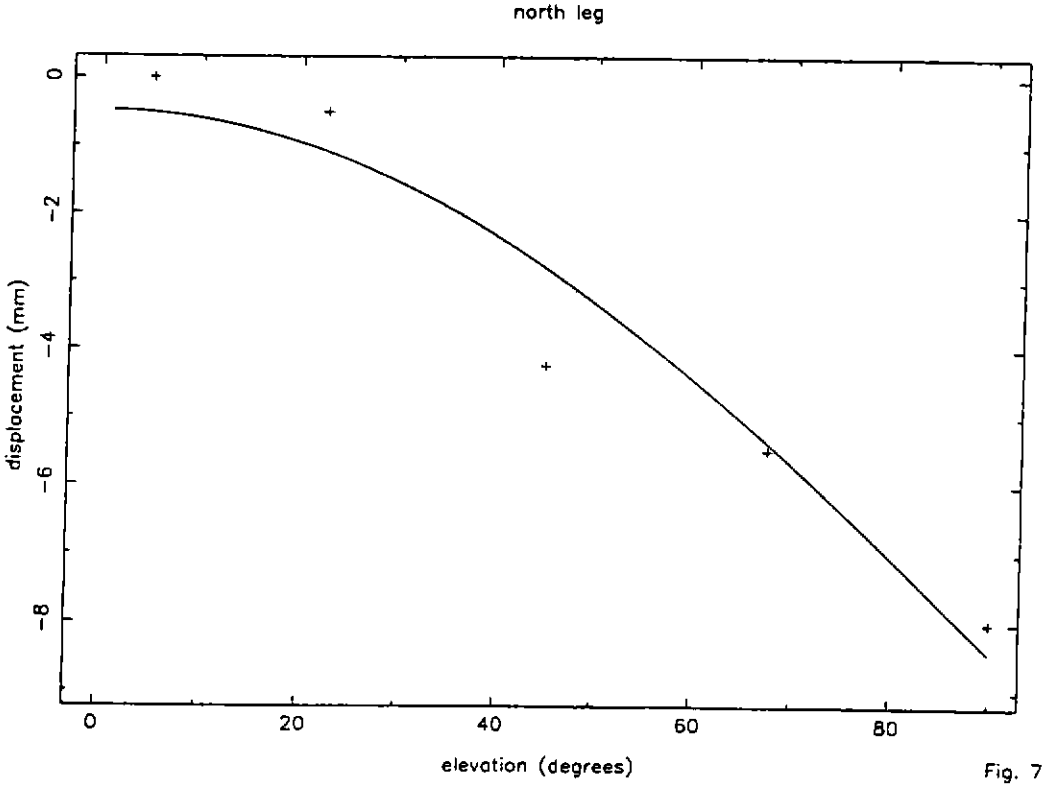
north leg
displacement (mm)
0
-2
-4
-6
-8
0
20
40
60
80
elevation (degrees)

Fig. 7